Letters

An Adaptive Dual-Loop Lyapunov-Based Control Scheme for a Single-Phase UPS Inverter

Jinsong He, *Student Member, IEEE*, Chan Chok You, *Member, IEEE*, Xin Zhang, *Senior Member, IEEE*, Zhan Li, *Member, IEEE*, and Zhangjie Liu, *Member, IEEE*

***Abstract*—This letter proposes an adaptive Lyapunov-based control strategy for a single-phase uninterruptible power supply inverter with inherent dual control loops. The control law is derived via a proposed Lyapunov function which takes both dual-loop requirements and the global large-signal stability demand into account. Besides, in the proposed control scheme, the load disturbance is suppressed adaptively without any additional load-current sensors or observers. The load voltage is regulated with better steady-state and dynamic performance, as well as with great robustness against the parametric variations. Finally, experimental results verify the effectiveness of the proposed control scheme.**

***Index Terms*—Control, large-signal stability, Lyapunov, robustness, steady-state and dynamic, uninterruptible power supply (UPS).**

Nomenclature

E	DC-link voltage.
f_s	Switching frequency.
ω	Fundamental angular frequency.
L	Nominal filter inductance.
C	Nominal filter capacitance.
v_{ref}	Load voltage reference.
P	Output active power.
$i_{L\text{ref}}$	Inductor current reference.
i_L	Inductor current.
i_o	Load current.
e_1	Load voltage tracking error.
e_2	Inductor current tracking error.
$\tilde{\varepsilon}$	Virtual load estimating error.
Z	Load impedance (complex).
V	Lyapunov function.
μ	Switching function.

Manuscript received November 15, 2019; revised December 18, 2019; accepted January 25, 2020. Date of publication February 17, 2020; date of current version May 1, 2020. *(Corresponding author: Xin Zhang.)*

Jinsong He, Chan Chok You, Zhan Li, and Zhangjie Liu are with the School of Electrical and Electronic Engineering, Nanyang Technological University, Singapore 639798, Singapore (e-mail: jinsong001@e.ntu.edu.sg; ecychan@ntu.edu.sg; lizhan@zju.edu.cn; zhangjieliu@csu.edu.cn).

Xin Zhang is with the College of Electrical Engineering, Zhejiang University, Hangzhou 310027, China, and was with the School of Electrical and Electronic Engineering, Nanyang Technological University, Singapore 639798, Singapore (e-mail: jackzhang@ntu.edu.sg).

Color versions of one or more of the figures in this article are available online at http://ieeexplore.ieee.org.

Digital Object Identifier 10.1109/TPEL.2020.2974548

I. Introduction

Single-phase inverter with an *LC* output filter has been widely utilized in the uninterruptible power supply (UPS) systems. In order to ensure pure sinusoidal output voltage with great power quality and fast transient response under load disturbance, numerous linear and nonlinear control schemes are intensively studied.

Cascaded proportional integral (PI)/proportional resonant (PR) control is commonly used in linear control approaches. According to the internal model principle, PI control in the stationary reference frame follows the sinusoidal reference accompanied by steady-state errors, while PR control could track the sinusoidal command accurately. Deadbeat control ensures fast dynamic response while it is inherently sensitive to parametric variations [1]. Sliding-mode control is robust against the parametric variations but suffers from the chattering phenomenon [2]. Repetitive control is an expert at tracking/rejecting periodic reference/disturbance but it has comparatively large intersample ripples [3]. Model predictive control achieves great transient response at the expense of a relatively large computation burden and varying switching frequency [4]. In [5], a hybrid dual-loop control is proposed, embedded with the PI control, the repetitive control, and the feedforward control. This approach requires complicated individual design stages. In [6], H-infinity control is investigated, which could theoretically ensure control robustness under specific premises.

The above-mentioned control strategies have case-by-case strengths and limitations, but one limitation they have in common is that the global large-signal stability of the system cannot be rigorously guaranteed. In fact, it is a concern for the system when exposed to large perturbations away from the operating point.

To this end, Lyapunov-based control schemes emerge. The conventional approach formulates a Lyapunov function (V) as the sum of linear-quadratic tracking errors associated with the capacitor voltage and the inductor current. Then, the final control law is selected to assure the negative definiteness of dV/dt. However, it inherently yields out a single-current-loop control

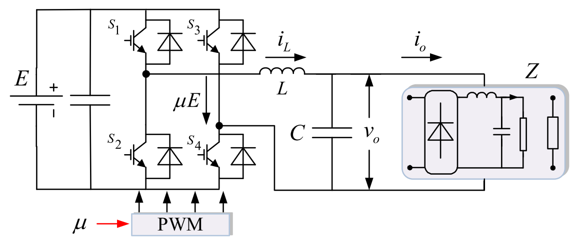

Fig. 1. Investigated single-phase UPS inverter.

scheme [7]–[10]. For an islanded inverter application, it leads to a steady-state error and slack dynamic response [10]. To fix this problem, Sefa *et al*. [7]–[10] extend the conventional single-loop control to a dual-loop counterpart via an artificial importation of capacitor voltage feedback. However, this action inevitably requires afterward modification of the Lyapunov-based control law, which cannot rigorously guarantee the negative definiteness of d*V*/d*t* unconditionally. This strategy also needs one load current sensor for practical implementation. As an economical alternative, the load current sensors are replaced by observers [4], [11], while the observer and controller design indeed require two separate design stages. Observer optimization complicates the controller design, which correlates with Riccati equation solving bandwidth allocation based on Kalman filter theory.

Therefore, current research on Lyapunov-based control schemes for the system is still on the way. Aiming to address the above-mentioned obstacles, an adaptive dual-loop Lyapunov-based control strategy is proposed in this letter. The proposed approach inherently has dual control loops with no need to import the voltage control loop artificially. Thus, global large-signal stability of the system can be rigorously guaranteed. Meanwhile, load disturbance can be suppressed adaptively without any additional load-current sensors or observers. The test results show that the proposed control scheme brings better steady-state and dynamic performance to the inverter with good robustness against the parameter variations.

II. Mathematical Modeling

A. Average Model of the Investigated System

According to KCL/KVL, the average model of the system, as shown in Fig. 1, can be represented as

$$L\mathrm{d}i_L/\mathrm{d}t = \mu \cdot E - v_o \tag{1}$$

$$C\mathrm{d}v_o/\mathrm{d}t = i_L - i_o \tag{2}$$

where system parameters are denoted as filter inductance *L*, filter capacitance *C*, dc-link voltage *E*, switching function μ, inductor current i_L, load voltage v_o, and load current i_o.

B. Load Voltage Reference v_{ref}

The investigated system is bound to reach the equilibrium point in steady state, where v_o will track v_{ref}, given by

$$v_{\mathrm{ref}} = v_m \sin(\omega t)\,. \tag{3}$$

Here, v_m denotes the load voltage reference amplitude.

C. Current-Loop Reference i_{ref}

Substituting v_{ref} into (2), expression of the current-loop reference i_{ref} can be found as follows:

$$i_{\mathrm{ref}} = \omega C v_m \cos(\omega t) + i_o. \tag{4}$$

D. Model of the Load Current i_o

As shown in (4), the load current i_o is indispensable to configure i_{ref}. Accurate i_o can be expressed as

$$i_o = v_o/Z \rightarrow v_{\mathrm{ref}}/Z \tag{5}$$

where *Z* is the load impedance.

Since *Z* is an unknown complex, susceptible to uncertainty and nonlinearity, using (5) to calculate i_o is impossible in practice. Load current in this letter is estimated online via following adaptive law:

$$\hat{i}_o = v_{\mathrm{ref}}\hat{\varepsilon} \tag{6}$$

where $\hat{\varepsilon}$ is defined to replace the unknown 1/*Z* for the purpose of load disturbance suppression, whose detailed derivation will be given in Section II.

III. Proposed Adaptive Dual-Loop Lyapunov-Based Control Scheme

A. Proposed Lyapunov Function

An all-in-one modified Lyapunov function is proposed to derive out the final control law μ and expression of $\hat{\varepsilon}$ as follows:

$$V = \frac{1}{2}\left(L{e_1}^2 + C{e_2}^2\right) + \frac{1}{2}\tilde{\varepsilon}^2\Big/\gamma \tag{7}$$

where e_1 is the current-loop tracking error and e_2 is the voltage-loop tracking error. e_1 and e_2 are defined in (8) and (9), respectively. In addition, $\tilde{\varepsilon}$ is defined as the virtual tracking error resulted from load disturbance, which is defined in (10). γ is an artificially imported controller parameter ($0 < \gamma < 1$).

$$e_1 = i_L - i_{\mathrm{ref}} \tag{8}$$

$$e_2 = v_o - v_{\mathrm{ref}} \tag{9}$$

$$\tilde{\varepsilon} = \hat{\varepsilon} - 1/Z. \tag{10}$$

B. Derivation of the Adaptive Dual-Loop Control Law

If (7) reached the equilibrium, (8)–(10) would have converged to zero, whose behavior around the equilibrium point (e_1, e_2, $\tilde{\varepsilon} = 0$) is investigated via Lyapunov's direct method. It points out that the equilibrium point is globally asymptotically stable unless *V* satisfies the following three premises:

1) I: $V \geq 0$, where $V = 0$ if and only if e_1, e_2, $\tilde{\varepsilon} = 0$;
2) II: $V \rightarrow \infty$ if any of e_1, e_2, $\tilde{\varepsilon} \rightarrow \infty$;
3) III: d*V*/d*t* < 0 for all points except the equilibrium point.

Premises I and II can be inherently fulfilled according to the positive definite expression of (7). To examine whether Premise III holds or not, the expression d*V*/d*t* requires to be derived out

$$\mathrm{d}V/\mathrm{d}t = Le_1\dot{e}_1 + Ce_2\dot{e}_2 + \tilde{\varepsilon}\dot{\tilde{\varepsilon}}/\gamma. \tag{11}$$

To represent (11), derivatives of (8)–(10) should be figured out. According to (1), (2), and (5), it is nor far to seek out that

$$\dot{e}_1 = [\mu \cdot E - (v_{\text{ref}} + e_2)] / L - \dot{i}_{\text{ref}} \tag{12}$$

$$\dot{e}_2 = [i_{\text{ref}} + e_1 - (v_{\text{ref}} + e_2) / Z] / C - \omega v_m \cos(\omega t) \tag{13}$$

$$\dot{\tilde{\varepsilon}} = \mathrm{d}\tilde{\varepsilon}/\mathrm{d}t = \dot{\hat{\varepsilon}} = \mathrm{d}\hat{\varepsilon}/\mathrm{d}t. \tag{14}$$

As shown in (12), the expression of $\mathrm{d}i_{\text{ref}}/\mathrm{d}t$ is further required. To this end, substituting (6) into (4). Then, the modified i_{ref} incorporated with $\hat{\varepsilon}$ will be represented as

$$i_{\text{ref}} = \omega C v_m \cos(\omega t) + v_{\text{ref}}\hat{\varepsilon}. \tag{15}$$

Taking first-order time derivative of (15), it gives

$$\mathrm{d}i_{\text{ref}}/\mathrm{d}t = \dot{i}_{\text{ref}} = v_{\text{ref}}\left(\dot{\hat{\varepsilon}} - \omega^2 C\right) + \omega v_m \cos(\omega t)\,\hat{\varepsilon}. \tag{16}$$

Subsequently, substituting (12)–(16) into (11), it yields out (17) shown at the bottom of this page, which demonstrates that $\mathrm{d}V/\mathrm{d}t = \alpha + \beta + \chi$, where α, β, and χ are expressed as

$$\alpha = -\sigma {e_1}^2 - 1/Z \cdot {e_2}^2 < 0 \tag{18}$$

$$\beta = \left(v_{\text{ref}} e_2 + \dot{\hat{\varepsilon}}/\gamma\right)\tilde{\varepsilon} \tag{19}$$

$$\chi = \left[\mu E - \left(1 + \omega^2 LC - L\dot{\hat{\varepsilon}}\right) v_{\text{ref}} - \omega L v_m \cos(\omega t)\,\hat{\varepsilon} + \sigma e_1\right] e_1. \tag{20}$$

As shown in (17), $-\sigma {e_1}^2$ is contained in α, whose counterpart $+\sigma {e_1}^2$ is embedded in χ, so that $\mathrm{d}V/\mathrm{d}t$ remain unchanged. This action leads to the importation of $-\sigma e_1$ in later (23). σ is another controller parameter ($\sigma > 0$).

Since $\alpha < 0$ has been inherently guaranteed, premise III can be satisfied if $\beta = 0$ and $\chi = 0$, which leads to $\mathrm{d}V/\mathrm{d}t = \alpha < 0$. By setting $\beta = 0$, it gives

$$\dot{\hat{\varepsilon}} = -\gamma v_{\text{ref}} e_2. \tag{21}$$

Thus, the formula of the adaptive term $\hat{\varepsilon}$ can be finally expressed as

$$\hat{\varepsilon} = \int \dot{\hat{\varepsilon}} dt = \int -\gamma v_{\text{ref}} e_2 dt. \tag{22}$$

The above-mentioned integrator ($\int$) will not stop working until the equilibrium point has been reached, where $e_2 \to 0$.

According to (20), $\chi = 0$ can be guaranteed if the final control law is selected as

$$\mu = \left[\left(1 - \omega^2 LC + L\dot{\hat{\varepsilon}}\right) v_{\text{ref}} + \omega L v_m \cos(\omega t)\,\hat{\varepsilon} - \sigma e_1\right] \Big/ E. \tag{23}$$

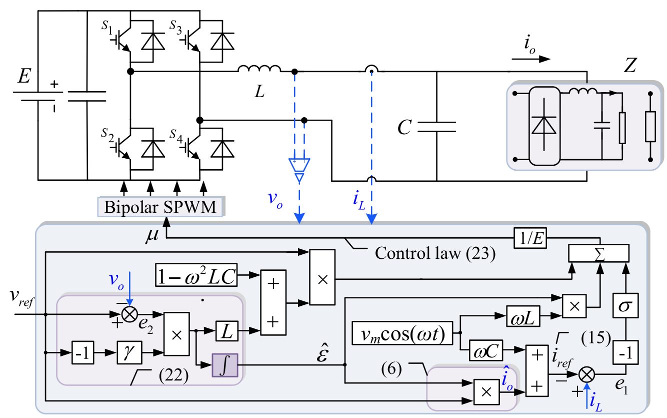

Fig. 2. Proposed adaptive dual-loop Lyapunov-based control scheme.

C. Implementation of Proposed Control Scheme

According to (21)–(23), the control block of the proposed control strategy is sketched in Fig. 2. As seen, the proposed control scheme inherently has dual control loops (e_1 and e_2 are contained). In addition, none of the additional load-current sensors or observers is required in Fig. 2.

Note that the proposed adaptive Lyapunov-based control is specially devised for single-phase UPS applications. When extended for grid-connected application and multiple inverters' parallel operation, a separate derivation for the topology of a specific system is required, where a seamless transition technique is commonly used [12].

IV. Stability Analysis and Robustness Verification

A. Stability Analysis

Substituting (21)–(23) into (12)–(14), the error dynamics of the regulated closed-loop system would be expressed as

$$\dot{x} = A(t)\,x \tag{24}$$

where $x = [e_1, e_2, \tilde{\varepsilon}]^T$, and

$$A(t) = \begin{pmatrix} -\sigma/L & -1/L & 0 \\ 1/C & -1/ZC & v_m \sin(\omega t)/C \\ 0 & -\gamma v_m \sin(\omega t) & 0 \end{pmatrix}. \tag{25}$$

It demonstrates that $A(t) = A(t + T)$ where $T = 0.02$ s. Thus, (24) is a linear time periodic system [13]. Taking an equivalent

$$\mathrm{d}V/\mathrm{d}t = \underbrace{-\sigma {e_1}^2 - 1/Z \cdot {e_2}^2}_{\alpha} + \underbrace{\left(v_{\text{ref}} e_2 + \dot{\hat{\varepsilon}}/\gamma\right)\tilde{\varepsilon}}_{\beta} + \underbrace{\left[\mu E - \left(1 + \omega^2 LC - L\dot{\hat{\varepsilon}}\right) v_{\text{ref}} - \omega L v_m \cos(\omega t)\,\hat{\varepsilon}\right] e_1 + \sigma {e_1}^2}_{\chi} \tag{17}$$

transformation of $A(t)$, expressed as

$$A(t) = \begin{pmatrix} L^{-1} & 0 & 0 \\ 0 & C^{-1} & 0 \\ 0 & 0 & \gamma \end{pmatrix} \times \underbrace{\begin{pmatrix} -\sigma & -1 & 0 \\ 1 & -Z^{-1} & v_m \sin(\omega t) \\ 0 & -v_m \sin(\omega t) & 0 \end{pmatrix}}_{M}. \tag{26}$$

Taking a linear equivalent transformation of x, it gives

$$y = P_T x \tag{27}$$

where P_T is a nonsingular diagonal matrix, given by

$$P_T = \begin{pmatrix} L^{1/2} & 0 & 0 \\ 0 & C^{1/2} & 0 \\ 0 & 0 & \gamma^{-1/2} \end{pmatrix}. \tag{28}$$

Then, (24) will be transformed into

$$\dot{y} = P_T \cdot A(t) \cdot {P_T}^{-1} y. \tag{29}$$

Since matrix P_T is nonsingular, the stability of system (29) is equivalent to that of (24). Substituting (26) into (29), it gives

$$\dot{y} = {P_T}^{-1} \cdot M \cdot {P_T}^{-1} y. \tag{30}$$

A Lyapunov function V_2 is formulated to prove the large-signal stability of the system, given by

$$V_2(y) = y^H y \tag{31}$$

where y^H is the conjugate transpose matrix of y. The derivative of (31) is expressed as

$$\mathrm{d}V_2/\mathrm{dt} = y^H \dot{y} + \dot{y}^H y. \tag{32}$$

Substituting (30) into (32), it yields out

$$\begin{aligned} \mathrm{d}V_2/\mathrm{dt} &= y^H \left({P_T}^{-1} \cdot M \cdot {P_T}^{-1} y\right) \\ &\quad + \left({P_T}^{-1} \cdot M \cdot {P_T}^{-1} y\right)^H y \\ &= y^H \Big[{P_T}^{-1} \cdot M \cdot {P_T}^{-1} + \left({P_T}^{-1}\right)^H \\ &\quad \cdot M^H \cdot \left({P_T}^{-1}\right)^H\Big] y. \end{aligned} \tag{33}$$

According to (28), $({P_T}^{-1})^H = {P_T}^{-1}$. Thus, (33) can be written as

$$\mathrm{d}V_2/\mathrm{dt} = y^H {P_T}^{-1} \left(M + M^H\right) {P_T}^{-1} y. \tag{34}$$

Substituting M, P_T into (34), $M + M^H$ cancel out all the off-diagonal entries of M and M^H, which gives

$$\mathrm{d}V_2/\mathrm{dt} = y^H \begin{pmatrix} -2\sigma L^{-1} & 0 & 0 \\ 0 & -\left[1/Z + (1/Z)^H\right] C^{-1} & 0 \\ 0 & 0 & 0 \end{pmatrix} y. \tag{35}$$

TABLE I
NOMINAL SYSTEM PARAMETERS

E	ω	f_s	L	C	P	v_m
350 V	100π	10 *k*Hz	1 *m*H	10 μF	5 *k*W	220×1.414 V

Note that $1/Z$ is the generalized load admittance, denoted as

$$1/Z = G + Bj \tag{36}$$

where $G > 0$ and B is arbitrary. Substituting (36) into (35), it yields out

$$\mathrm{d}V_2/\mathrm{dt} = y^H \begin{pmatrix} -2\sigma L^{-1} & 0 & 0 \\ 0 & -2GC^{-1} & 0 \\ 0 & 0 & 0 \end{pmatrix} y < 0. \tag{37}$$

It shows that the filter will not affect the global large-signal stability using the proposed control method provided that $\sigma > 0$ and $G > 0$. In fact, this condition can be easily satisfied, and σ, L, C, and Z could vary at a rather large range without deteriorating the system stability.

Owning to γ, v_m are located at the off-diagonal entries of $A(t)$, they mainly affect the system damping. While L, C, Z, and σ are located at the diagonal entries of (35), they will affect the dynamic response of the system.

Larger σ will result in higher convergence speed of the error dynamics, leading to better dynamic response. Smaller γ will provide more damping for the system. For system parameters specified in Table I, σ (20–2000) and γ (0.01–0.05) are their recommended selection range in this example case.

B. Robustness Against Plant Parametric Variations

To evaluate the robustness of the proposed approach, simulations are conducted under reference step and parametric variations where σ and γ are set as 200 and 0.05, respectively. As shown in Fig. 3, the stability of the system does not get deteriorated even under such a large scale of parametric variations. Estimated load currents in Fig. 3(a)–(d) are just slightly different, and the load voltage always remains pure sinusoidal.

V. EXPERIMENTAL RESULTS

A single-phase UPS inverter with an *LC* output filter has been fabricated for experimental verification, as seen in Fig. 4. The dSPACE 1103 is utilized as the controller. Plant parameters are the same as those used in Section IV-B.

A. Steady-State and Dynamic Performance Evaluation

Experiments are conducted to test the performance of the proposed control method when supplying the linear resistive load and nonlinear rectifier load, as shown in Fig. 5.

The test results of the single-phase UPS inverter have been shown in Fig. 6. In Fig. 6(a), linear resistive load steps from 500 W to 5 kW. In Fig. 6(b), load voltage reference first steps from 220 to 110 Vrms with 10 Ω linear resistive load. Then, it is restored to 220 Vrms again. In Fig. 4(c), nonlinear rectifier load steps from 200 W to 2 kW. As seen, the proposed control scheme

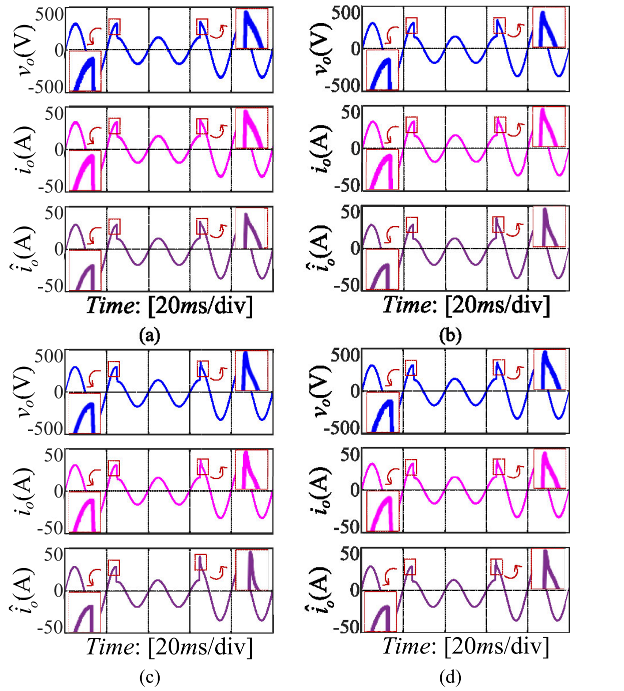

Fig. 3. Robustness against reference steps and plant parametric variations. (a) −50% L, −50% C. (b) +50% L, −50% C. (c) +50% L, +50% C. (d) −50% L, +50% C.

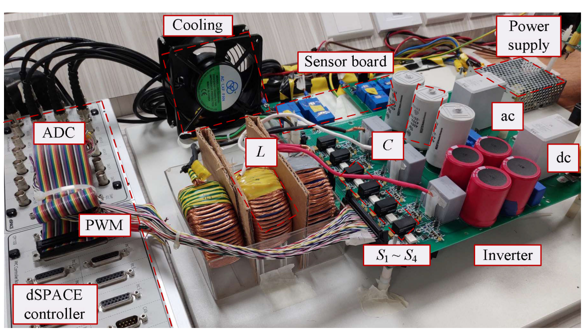

Fig. 4. Experimental setup.

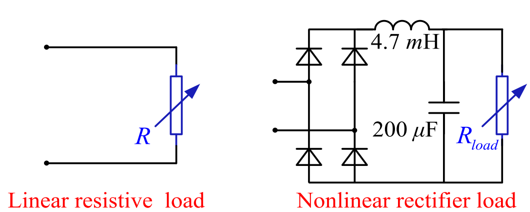

Fig. 5. Linear and nonlinear load used to do experiments.

regulates the load voltage with great steady-state and dynamic response under the scenario of a linear load step, reference step, and nonlinear rectifier load step.

B. Overload and Recovery Scenario

As shown in Fig. 7, the single-phase UPS inverter initially operates with 100% P linear resistive load. Then, 200% P overload happens. After two fundamental periods, the system goes into

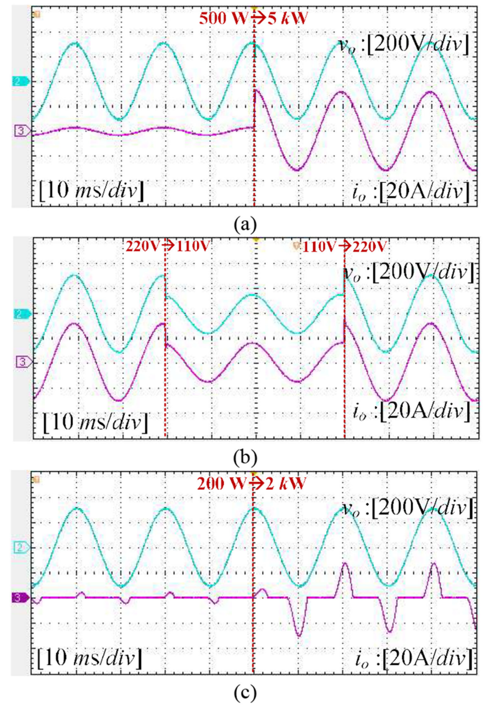

Fig. 6. Experimental waveforms with the proposed control method. (a) Resistive load step. (b) Voltage reference step with resistive load. (c) Nonlinear rectifier load step.

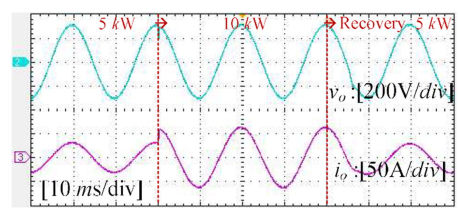

Fig. 7. Experimental waveforms with the proposed control method under overload and recovery process.

the recovery process (200% $P \rightarrow$100% P). The regulated load voltage almost remains sinusoidal even under the scenario of overload and recovery, which shows that the proposed adaptive control has great robustness against load disturbance.

VI. Conclusion and Future Work

In this letter, an adaptive Lyapunov-based control scheme is proposed for a single-phase UPS inverter, which not only has inherent dual control loops to ensure better steady-state and dynamic performance but also can rigorously guarantee the global large-signal stability. The detailed control law derivation is presented. The corresponding stability analysis and robustness verification are also discussed in this letter. Furthermore, with this control scheme, the load disturbance can be suppressed adaptively without any additional load-current sensors or observers. The experimental results eventually verify the effectiveness of the proposed control scheme. In our future work, the proposed control scheme is expected to be extended for grid-connected application and multiple inverters' parallel operation.

REFERENCES

[1] M. Pichan, H. Rastegar, and M. Monfared, "Deadbeat control of the stand-alone four-leg inverter considering the effect of the neutral line inductor," *IEEE Trans. Ind. Electron.*, vol. 64, no. 4, pp. 2592–2601, Apr. 2017.

[2] A. M.-Pastor, E. V.-Idiarte, A. C.-Pastor, and L. M.-Salamero, "Interleaved digital power factor correction based on the sliding-mode approach," *IEEE Trans. Power Electron.*, vol. 31, no. 6, pp. 4641–4653, Jun. 2016.

[3] G. Escobar, A. A. Valdez, J. L.-Ramos, and P. Mattavelli, "Repetitive-based controller for a UPS inverter to compensate unbalance and harmonic distortion," *IEEE Trans. Ind. Electron.*, vol. 54, no. 1, pp. 504–510, Feb. 2007.

[4] P. Cortés, G. Ortiz, J. I. Yuz, J. Rodríguez, S. Vazquez, and L. G. Franquelo, "Model predictive control of an inverter with output LC filter for UPS applications," *IEEE Trans. Ind. Electron.*, vol. 56, no. 6, pp. 1875–1883, Jun. 2009.

[5] Y. G. Gao, F. Y. Jiang, J. C. Song, L. J. Zheng, F. Y. Tian, and P. L. Geng, "A novel dual closed-loop control scheme based on repetitive control for grid-connected inverters with an LCL filter," *ISA Trans.*, vol. 74, pp. 194–208, 2018.

[6] M. A. Chowdhury, "Dual-loop H_∞ controller design for a grid-connected single-phase photovoltaic system," *Sol. Energy*, vol. 139, pp. 640–649, 2016.

[7] I. Sefa, S. Ozdemir, H. Komurcugil, and N. Altin, "An enhanced Lyapunov-function based control scheme for three-phase grid-tied VSI with LCL filter," *IEEE Trans. Sustain. Energy*, vol. 10, no. 2, pp. 504–513, Apr. 2019.

[8] H. Komurcugil, I. Sefa, N. Altin, and S. Ozdemir, "Lyapunov-function and proportional-resonant-based control strategy for single-phase grid-connected VSI with LCL filter," *IEEE Trans. Ind. Electron.*, vol. 63, no. 5, pp. 2838–2849, May 2016.

[9] I. Sefa, S. Ozdemir, H. Komurcugil, and N. Altin, "Comparative study on Lyapunov-function-based control schemes for single-phase grid-connected voltage-source inverter with LCL filter," *IET Renew. Power Gener.*, vol. 11, no. 11, pp. 1473–1482, Sep. 2017.

[10] H. Komurcugil, N. Altin, S. Ozdemir, and I. Sefa, "An extended Lyapunov-function-based control strategy for single-phase UPS inverters," *IEEE Trans. Power Electron.*, vol. 30, no. 7, pp. 3976–3983, Jul. 2015.

[11] E.-K. Kim, F. Mwasilu, H. H. Choi, and J.-W. Jung, "An observer-based optimal voltage control scheme for three-phase UPS systems," *IEEE Trans. Ind. Electron.*, vol. 62, no. 4, pp. 2073–2081, Apr. 2015.

[12] D. S. Ochs, B. Mirafzal, and P. Sotoodeh, "A method of seamless transitions between grid-tied and stand-alone modes of operation for utility-interactive three-phase inverters," *IEEE Trans. Ind. Appl.*, vol. 50, no. 3, pp. 1934–1941, May/Jun. 2014.

[13] N. M. Wereley, "Analysis and control of linear periodically time varying systems," Ph.D. dissertation, Dept. Aeronaut. Astronaut., Massachusetts Inst. Technol., Cambridge, MA, USA, 1990.